Journal Pre-proofs

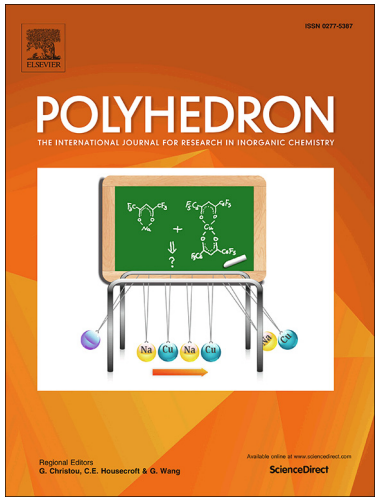

Photophysical, photochemical and DNA binding studies of prepared phthalocyanines

Arif Baran, Sumeyye Çol, Emel Karakılı ç, Furkan Özen

PII: S0277-5387(19)30650-3
DOI: https://doi.org/10.1016/j.poly.2019.114205
Reference: POLY 114205

To appear in: *Polyhedron*

Received Date: 15 September 2019
Revised Date: 19 October 2019
Accepted Date: 23 October 2019

Please cite this article as: A. Baran, S. Çol, E. Karakılı ç, F. Özen, Photophysical, photochemical and DNA binding studies of prepared phthalocyanines, *Polyhedron* (2019), doi: https://doi.org/10.1016/j.poly.2019.114205

This is a PDF file of an article that has undergone enhancements after acceptance, such as the addition of a cover page and metadata, and formatting for readability, but it is not yet the definitive version of record. This version will undergo additional copyediting, typesetting and review before it is published in its final form, but we are providing this version to give early visibility of the article. Please note that, during the production process, errors may be discovered which could affect the content, and all legal disclaimers that apply to the journal pertain.

© 2019 Published by Elsevier Ltd.

Journal Pre-proofs

MANUSCRIPT

Photophysical, photochemical and DNA binding studies of prepared phthalocyanines

Arif Baran*, Sumeyye Çol, Emel Karakılıç, Furkan Özen

Sakarya University, Faculty of Arts and Sciences, Chemistry Department, 54187, Sakarya, Turkey

abaran@sakarya.edu.tr

ABSTRACT

In this study, three phthalocyanine derivatives (M= Zn, Co, and metal-free) were synthesized using the corresponding ligand 4-(2-(4-(tert-butyl)phenoxy)ethoxy)phthalonitrile **2** in peripheral position, which was prepared from the reaction of 4-nitrophthalonitrile with 2-(4-(tert-butyl)phenoxy)ethan-1-ol **1**. Metallophthalocyanine (MPc) and Metal-free phthalocyanine (H_2Pc) derivatives, which have soluble groups in peripheral positions were synthesized. They are have high soluble in organic solvents depending on the appropriate position such as (tetrahydrofuran (THF), chloroform ($CHCl_3$), methylene chloride (DCM), acetone (ACE), Dimethyl formamide (DMF), and dimethylsulphoxide (DMSO))….etc. The structures of Metallophthalocyanine (MPc) and Metal-free phthalocyanine (H_2Pc) compounds **3a**, **3b**, and **3c** were characterized using UV–vis spectroscopy, infrared (FT-IR) spectroscopy, and MALDI-TOF MS. Additionally, DNA binding, metal chelating effect assay, and DPPH [2,2-diphenyl-1-picrylhydrazyl hydrate] radical scavenging assay of MPcs H_2Pc were investigated. In the interaction between Pc and CT-DNA the intrinsic binding constant (Kb) calculation was gave. Although the phthalocyanine compounds (**3a**, **3b** and **3c**) shoved low iron-containing iron chelating properties compared to EDTA, they can be said to have high metal chelating properties at the specified concentrations for this phthalocyanines. The DPPH radical scavenging activity of Pcs was elucidated according to the estimation of their in vitro antioxidant activities.

Keywords: Photodegradation, Singlet oxygen, Binding properties, Photophysical and Photochemical investigation

Journal Pre-proofs

1. Introduction

Phthalocyanines (Pcs) and their derivatives are important molecules and thus extensive studies on Pcs have been going on for many years. Hitherto Pcs and their derivatives have had many potential applications in material science, including chemical sensors, liquid crystals, Langmuir–Blodgett films [1-3] and sensitizers for photodynamic therapy of cancer [4,5]. Moreover, they are also known for their good conductive properties such as in optical components for nonlinear optics [6,7]. The unknown additional properties of these molecules will be discovered in time. As the properties of such molecules are being discovered, world-class chemists are taking interest in the more fascinating features of Pcs [8,9].

Because of intermolecular interactions between peripherally unsubstituted Pcs they have a solubility problem in organic solvents [10]. If the solubility of the synthesized Pc is low in organic solvents, in this case it undergoes aggregation and this solubility problem limits its use [11] To overcome this problem of solubility and aggregation, the substituent must be chosen meticulously. Introduction of tri- or tetra-substituent groups into the periphery of the Pc framework can minimize the solubility problem by increasing the distance between atoms in the porphyrin skeleton. In connection with the formation of constitutional isomers and high dipole moment that results from the unsymmetrical arrangement of the substituents at the periphery, tetra-substituted Pcs exhibit better solubility and lower aggregation than the corresponding octa-substituted Pcs [12,13]. If there are substituents that are electron releasing in the peripheral or non-peripheral position of the Pc ring, it provides a bathochromic shift in the Q band. That is to say, a complex substituent in a peripheral position has a greater tendency to minimize aggregation than a complex substituent in a non-peripheral position [14].

In the present study, 2-(4-(tert-butyl) phenoxy) ethan-1-ol **1**, prepared first from the reaction of 4-(tert-butyl) phenol and ethylene carbonate, was reacted with 4-nitrophthalonitrile, which resulted in 4-(2-(4-(tert-butyl)phenoxy)ethoxy)phthalonitrile **2** as a good electron-donating system for the metallophthalocyanine (MPc) and metal-free phthalocyanine (H_2Pc). The reaction of 4-(2-(4-(tert butyl)phenoxy)ethoxy)phthalonitrile **2** with $Zn(OAc)_2.2H_2O$ and $Co(OAc)_2.4H_2O$, complex salts in DMF, using DBU catalytically at reflux temperature gave metallophthalocyanines (MPcs). Using the same condition (without using complex salts) gave the metal-free phthalocyanine (H_2Pc). Then these complexes were investigated in terms of DNA binding, metal chelating effect, and DPPH radical scavenging.

2. Material and methods

2.1. General procedures-materials and methods

The chemicals and solvents using in this study, (4-(tert-butyl)phenol, 1,3-dioxolan-2-one, 4-nitrophthalonitrile, K_2CO_3, 1,8-diazabicyclo[5.4.0]undec-7-ene (DBU), $Zn(OAc)_2.2H_2O$, and $Co(OAc)_2.4H_2O$), were purchased from Merck, Sigma Aldrich, Acros,…. The solutions used in the experiment (DMF, THF, DCM, DMSO, and ethanol) were dried and purified. For recording the NMR spectra 300 MHz (^{1}H NMR) and 75 MHz (^{13}C NMR) spectrometers were used. The chemical shifts were given in ppm (δ) relative to internal tetramethylsilane (TMS, δ 0.0 ppm) or with the solvent reference relative to TMS employed as the internal standard ($CDCl_3$, δ 7.26 ppm and CD_3OD, δ 3.35, 4.78 ppm or $(CD_3)_2SO$). An Ati Unicam Mattson 1000 Series FT-IR (ATR system) spectrometer was used for recording the IR spectra. The MALDI-TOF spectra were recorded with Bruker Daltonics flex Analysis. Photo-irradiation was conducted using a General Electric quartz line lamp (300 W). A Shimadzu UV 2600 model spectrophotometer was used for recording the UV–vis spectra. Fluorescence measurements and DNA-binding experiments were conducted with the Agilent Technologies Cary Eclipse spectrophotometer.

2.2. Synthesis

2.2.1. Synthesis of 2-(4-(tert-butyl)phenoxy)ethan-1-ol (1): 2-(4-(tert-butyl)phenoxy)ethan-1-ol (**1**) was prepared according to the method reported in the literature,[15] with some modifications. To 4-(tert-butyl)phenol (1.0 g, 6.66 mmol) in DMF was added the substituted 1,3-dioxolan-2-one (1.17 g, 13.31 mmol). After the mixture was stirred for 15 min, K_2CO_3 (1.84 g, 13.31 mmol) was added. Then the stirring solution was refluxed for 24 h. The completion of the reaction was checked by TLC, the mixture was added dropwise, and then ice water (250 mL) was added, followed by shaking. The inorganic layer was eluted off. The organic phase was washed with plenty of water, dried on Na_2SO_4, and evaporated to give light brown liquid (1.04 g, 80% yield). MW: 194.27. FT-IR max/cm^{-1}: 3367 cm^{-1} (OH), 3040 cm^{-1} (Ar–H); 2959, 2904 cm^{-1} (aliphatic C-H); 1609, 1580, 1512 cm^{-1} (Ar–C=C); 1040 cm^{-1} (C-O-C). ^{1}H-NMR (300 MHz, CD_3OD): 7.33 (2H, d, H4), 6.88 (2H, d, H5), 4.08 (2H, t, H7), 3.95 (2H, t, H8), 2.33

(H, s, OH), and 1.31 (9H, s, H1). ^{13}C-NMR (75 MHz, CD_3OD): 156.56 C6, 144.07 C3, 126.56 C4, 114.25 C5, 69.39 C7, 61.75 C8, 34.34 C2, and 31.76 C1.

2.2.2. Synthesis of 4-(2-(4-(tert-butyl)phenoxy)ethoxy)phthalonitrile (2): To a mixture of 4-nitrophthalonitrile (0.7 g, 3.60 mmol) in 15 mL of dry DMF was added 2-(4-(tert-butyl)phenoxy)ethan-1-ol (0.62 g, 3.60 mmol) (**1**) and the resulting mixture was stirred at 50 °C under N_2. Then to the stirred solution was added anhydrous K_2CO_3 (0.5 g, 3.60 mmol) over 1 h. After stirring for a further 12 h, TLC was used to check that the reaction was completed. The insoluble residue was removed by filtration. The solution was added dropwise and then ice water (250 mL) was added, followed by shaking. Then the solution was washed with plenty of water, dried on Na_2SO_4, evaporated, and dried to give residue. The residue was subjected to column chromatography with silica gel, using different ratios of DCM/EtOAc to give a brown solid after evaporation of the collected filtrates (Yield: 0.85 g, 73%). Mp: 107-109 °C. FT-IR max/cm^{-1}: 3093 cm^{-1} (Ar–H); 2961, 2873 cm^{-1} (aliphatic C-H); 2232 cm^{-1} (C≡N); 1598, 1564, 1509 cm^{-1} (C=C) and 1099 cm^{-1} (C-O-C). ^{1}H-NMR (300 MHz, $CDCl_3$): δ ppm 7.73 (d, 1H, H13), 7.34-7.23 (m, 4H, H4, 10, 14), 6.87 (d, 2H, H5), 4.42 (t, 2H, H8), 4.35 (t, 2H, H7), and 1.29 (s, 9H, H1). ^{13}C-NMR (75 MHz, $CDCl_3$): 162.05 C9, 156.07 C6, 144.56 C3, 135.48 C13, 126.68 C4, 120.02 C14, 119.84 C10, 117.65 C11, 115.92 C15, 115.50 C16, 114.25 C5, 107.82 C12, 67.98 C8, 66.17 C7, 34.38 C2, and 31.74 C1.

2.2.3. Synthesis of zinc (II) phthalocyanine (3a): To compound **2** (0.2 g, 0.62 mmol) was added $Zn(OAc)_2.2.H_2O$ (0.095 g, 0.44 mmol) and a catalytic amount of 1.8-diazabicyclo[5.4.0]undec-7-ene (DBU) at rt. The stirred solution was heated to 130 °C using DMF as reaction solution under N_2. The reaction was stirred at this temperature for 24 h until the color turned dark green. After completion of the reaction, the temperature was lowered to room temperature. The insoluble salt was removed by filtration and the dark green product was poured into ice water (100 mL), stirred, and filtrated. The filtrate was then washed with hot water and dried in an open oven. Finally the filtrate was eluted on silica gel with ether and hexane/EtOAc 4:1 respectively for separation from the starting materials or unreacted materials. Then the undesired fractions were separated and filtered with tetrahydrofuran. The filtrate was evaporated using an evaporator to give a pure and readily soluble product in DCM, $CDCl_3$, THF, DMF, and DMSO. MW: 1346.95. Yield: 0.15 g (42%). Mp>350 °C. FT-IR ν_{max} (cm^{-1}): 3041 cm^{-1} (Ar–H); 2952, 2904 cm^{-1} (aliphatic C–H); 1606, 1583, 1511 cm^{-1} (C=N, C=C); 1041 cm^{-1} (C-O-C). UV–vis (DMF), λ_{max}, nm: 680, 612.5, 357.6. MALDI-TOF MS: m/z $[M]^+$ calcd.

Journal Pre-proofs

for $C_{80}H_{80}N_8O_8Zn$: 1346.95; found [M] 1346.93. Elemental analysis for [$C_{80}H_{80}N_8O_8Zn$]: C, 71.34; H, 5.99; N, 8.32. Found: C, 71.38; H, 5.96; N, 8.37%.

2.2.4. Synthesis of cobalt (II) phthalocyanine (3b): To compound **2** (0.2 g, 0.62 mmol) was added a mixture of $Co(OAc)_2.4H_2O$ (0.077 g, 0.44 mmol) and a catalytic amount of DBU, followed by stirring at 130 °C in dry DMF under N_2 for 24 h. At the end of this time, after the color of the reaction had turned green, the reflux temperature was reduced to room temperature. The insoluble residue was disposed of by filtration and the dark green solution in DMF was poured into ice-water (100 mL) and stirred. The precipitation phase was filtered and washed with hot water and warm ethanol. The dark blue residue was dried in an open oven and was separated from the starting materials or unreacted materials after purification on silica gel by column chromatography using a solution such as ether, hexane/ethylacetate, and tetrahydrofuran (THF). After the same fraction was collected and evaporated under reduced pressure, an easily soluble product was obtained in DCM, $CDCl_3$, THF, DMF, and DMSO. Yield: 0.18 g (50%). Mp>350 °C. MW: 1340.50. FT-IR ν_{max} (cm^{-1}): 3040 cm^{-1} (Ar-H); 2954, 2868 cm^{-1} (aliphatic C–H); 1608, 1512, 1479 cm^{-1} (C=N, C=C); 1094, 1066 cm^{-1} (C-O-C). UV–vis (DMF), λ_{max}, nm: 670.0, 609.5, 325.0. MALDI-TOF MS: m/z $[M]^+$ calcd. for $C_{80}H_{80}N_8O_8Co$: 1340.50; found [M] 1340.80. Elemental analysis for [$C_{80}H_{80}N_8O_8Co$]: C, 71.68; H, 6.02; N, 8.36. Found: C, 71.70; H, 6.05; N, 8.37%.

2.2.5. Synthesis of metal-free phthalocyanine (3c): To a mixture of **2** (0.2 g, 0.62 mmol) in absolute DMF was added a catalytic amount of DBU and the mixture was stirred at 130 °C in dry DMF for 24 h under N_2. After the change of the color to dark blue was complete the reaction mixture was cooled to room temperature. The insoluble salt was removed by filtration and the dark green product was poured into ice-water (100 mL) and stirred. After precipitation of the filtrates, the mixture was washed with water and warm ethanol, and the unreacted organic materials were removed. The dark blue product was dried in an open oven and chromatographed with ether, hexane/ethylacetate, and tetrahyrofuran to remove the starting materials or unreacted material. After collection and evaporation of the solution by evaporator gave pure **3c**; it is readily soluble in DCM, $CDCl_3$, THF, DMF, and DMSO. Yield: 0.15 g (48%). Mp>350 °C. MW: 1283.58. FT-IR ν_{max} (cm^{-1}): 3283 cm^{-1} (Ar-H); 2923, 2853 cm^{-1} (aliphatic C–H); 1735, 1607, 1479 cm^{-1} (C=N, C=C); 1238, 1097 cm^{-1}, (C-O-C). UV–vis (DMF), λ_{max}, nm: 703, 672, 644, 610, 397, 343. MALDI-TOF MS: m/z $[M]^+$ calcd. for $C_{80}H_{82}N_8O_8$: 1283.58.; found [M]

Journal Pre-proofs

1283.67. Elemental analysis for [$C_{80}H_{82}N_8O_8$]: C, 74.86; H, 6.44; N, 8.73. Found: C, 74.82; H, 6.47; N, 8.76%.

2.3. DNA Binding Study

2.3.1. DNA Binding assay:

The DNA solution was prepared as follows: 10 mg of CT-DNA was dissolved in 1.5 mL of 5 μM Tris-HCl/50 μM NaCl buffer. The UV absorption ratio of the CT-DNA solution is 1.85 at 260 and 280 nm, indicating that the DNA is sufficiently free from protein and single-stranded DNA. Using absorption spectroscopy the concentration of CT-DNA per nucleotide phosphate was calculated by its molar absorption coefficient value of 6600 M^{-1} cm^{-1} at 260 nm. The Pcs' (concentration was kept constant, 7.5 μM) electronic absorption spectrum was assessed before and after the addition of gradually increasing concentrations of DNA. The electronic absorption spectrum of Pcs was obtained in 1-cm quartz cuvettes, after 10 min incubation in 5 μM Tris-HCl/50 μM NaCl buffer, 5% DMSO (pH = 7.2) at 400-750 nm. The absorbance of DNA was eliminated by applying a reference cuvette containing an equal amount of DNA. In the interaction between Pc and CT-DNA the intrinsic binding constant (Kb) calculation was given as follows (Equal 1):

$$[DNA] / (\varepsilon a-\varepsilon f) = [DNA] / (\varepsilon b-\varepsilon f) + 1 / K_b (\varepsilon a-\varepsilon f) \quad (Eq.1)$$

Here εa = Absorption/[phthalocyanine] (the apparent), εa = extinction coefficient for the free phthalocyanine, εb = extinction coefficient for phthalocyanine in bound form. The [DNA] / (εb εf) is versus [DNA], K_b is given by the ratio of slope to the y intercept [16].

2.3.2. Metal Chelating Effects Assay

The metal chelating activities of Pcs were investigated by the iron ion-ferrozine method, compared to EDTA, which was used as reference compound [17]. To a solution of 50 μL of 2 mM $FeCl_2$ and 100 μL of 5 mM ferrozine was added 500 μL of varying concentrations (25–100 μM) of Pc. The optical density of samples at rt was recorded after 10 min incubation at 562 nm, The control assay of the mixture was also conducted without using Pc. All experiments were in

triplicate and the results recorded as the mean ± standard deviation (S.D.). The metal chelating effect was calculated as follows (Equal 2) [18].

Metal chelating effect (%): $[[A_{control} - A_{sample}]/A_{control}] \times 100$ (*Eq. 2*)

2.3.3. DPPH Radical Scavenging Assay

The DPPH radical scavenging activity of Pcs was elucidated according to the estimation of their in vitro antioxidant activities [19]. To the mixture of 0.5 mL of Pcs prepared at varying concentrations in DMSO was added a mixture of freshly prepared 1 mL of 0.1 mM DPPH in methanol. The incubation assay of the mixtures in the dark for 50 min at rt was performed and after this incubation time the optical density of the assay mixtures was recorded at 517 nm. In the same condition the control mixture (without Pcs) and gallic acid standard mixture were examined. All experiments were in triplicate and the results recorded as the mean ± S.D. The free radical scavenging effect of Pcs was calculated according to the above method (Equal 2).

3. Result and discussion

3.1. Synthesis and characterization

In the synthetic pathway, a well-established method for the synthesis of easily soluble tetrasubstituted MPcs and H_2Pc was implemented, which involved an aromatic nucleophilic substitution reaction occurring between 4-nitrophthalonitrile and 2-(4-(tert-butyl)phenoxy)ethan-1-ol **1**, followed by cyclic tetramerization using $Zn(OAc)_2.2H_2O$ and $Co(OAc)_2.4H_2O$ metal salt for MPcs and without using a metal salt for H_2Pc. The metallation reaction after reflux in DMF and using DBU (catalytically) afforded 42% yield for ZnPc and afforded 50% yield for CoPc. The same method without using metal salt afforded 48% yield of metal-free Pc. At the start of the reaction, different solvents (pentane-1-ol, DMSO, and DMF) with high boiling points were used for MPcs and H_2Pc. The efficiency of the reaction was higher in DMF. The MPcs and H_2Pc reactions were therefore carried out in DMF. For the purity of the product, different solution ratios were used but the only convenient solution was chosen as THF and acetone in 4:1 ratio and the purification was realized by column chromatography on silica gel.

Journal Pre-proofs

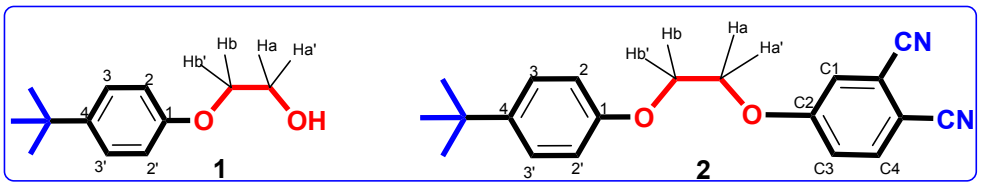

Figure 1. 2-(4-(tert-butyl)phenoxy)ethan-1-ol (**1**) and 4-(2-(4-(tert-butyl)phenoxy)ethoxy) phthalonitrile (**2**)

The characterization of the Pcs was performed by NMR, IR, UV-vis, and MALDI-TOF MS. The results of the analysis were compatible with the estimated structures. The proton NMR in $CDCl_3$ showed that the synthesized compounds were pure and that all protons occurred in their pending regions in the ring. In compound **1**, while aromatic protons (H-3 and H-3') resonated between 7.37 and 7.30 ppm (A part of an AA'BB' system), other aromatic protons (H2 and H2') resonated between 6.89 and 6.84 ppm (B part of an AA'BB' system. On the other hand, while methylenic protons (Ha and Ha') resonated at 4.07 ppm as multiplets, the other methylenic protons (Hb, Hb') resonated at 3.95 ppm, also as multiplets. The hydroxyl and methyl groups resonated as broad singlets at 2.19 ppm (for –OH group) and as singlets at 1.30 ppm (for methyl groups), respectively. The nine ^{13}C-NMR resonance signals are compatible with the prescribed structure in Scheme 1. In the configuration elucidation of compound **2**, the nitrile bound ring proton (Hc4) resonated as a multiplet giving the A part of an AA'BB' system at 7.70 ppm and the neighboring proton Hc3 resonated as a multiplet giving the B part of an AA'BB' system at 7.32 ppm. Another aromatic ring proton (Hc1) resonated as a multiplet at 7.31 ppm. For elucidation of the other part of a molecule, the H3 and H3' protons resonated as multiplets giving the A part of an AA'BB' system at 7.29 ppm, and the other protons (H2 and H2') resonated as multiplets giving the B part of an AA'BB' system at 6.86 ppm. Ethylenic protons Ha and Ha' or Hb and Hb' resonated as multiplets giving the A part of an AB system at 4.41 ppm and the other protons (Hb and Hb' or Ha and Ha') resonated as multiplets giving the B part of an AB system at 4.34 ppm. Methyl group protons resonated in their respective regions giving singlets at 1.29 ppm. In comparison with their theoretical result, the seventeen ^{13}C signals are consistent with the structure. In the course of the study, ^{1}H- and ^{13}C-NMR of the synthesized metallophthalocyanine (**3a**, **3b**) and metal-free Pc (**3c**) compounds could not be obtained even though different deuterium solvents were used (Scheme 1). NMR measurements of the CoPc (**3b)** was precluded owing to its paramagnetic nature, and the ZnPc (**3a**) and H_2Pc (**3c)** were not measured despite good solubility. However, all the mass spectra for phthalocyanines (**3a**, **3b, 3c)** confirmed the proposed cyclotetramerization.

Journal Pre-proofs

The IR spectra for compound **1** showed that while the hydroxyl group vibration appeared at 3450-3250 cm^{-1}, the aliphatic CH stretching vibration appeared at 2959-2869 cm^{-1}. However, the most convincing characteristic group is the etheric (C–O–C) bond vibration at ca. 1243–1245 cm^{-1} for **1**. In the IR spectra of compound **2**, the aliphatic CH stretching was shown at ca. 3074–2961 cm^{-1}, which resembles the aliphatic CH stretching of compound **1**. In addition, the most convincing feature is the presence of 2232 cm^{-1} vibrations in the cyano-functional group and the disappearance of the hydroxyl group. For the phthalocyanines (ZnPc, CoPc and H_2Pc) most convincing things is that the cyclotetramerization of the phthalonitrile derivatives with the disappearance of the CN three band at approximately 2232 cm^{-1}. Already three phthalocyanines (ZnPc, CoPc and H_2Pc) IR-spectra are close to each other.

In the MPc compounds (**3a**–**3b**) the UV–vis spectra are characteristic for the Q-band region, in this region at around 655-700 nm for MPc (**3a**) and 640-680 nm for MPc (**3b**) in DMF. The Soret band or B band is characteristic in the UV-vis spectra in the region at around 320-374 nm for MPc (**3a**) and at around <400 nm for MPc (**3b**). In the case of metal-free Pc Q_1 and Q_2 are characteristic at around 645-665 nm and 694-720 nm, while the B band is seen at around 320-380 nm. This is due to the π-π* transition of the Q band resulting from the HOMO (highest occupied molecular orbital) and the deepest π-π* transition of the B band originating from the LUMO (lowest unoccupied molecular orbital).

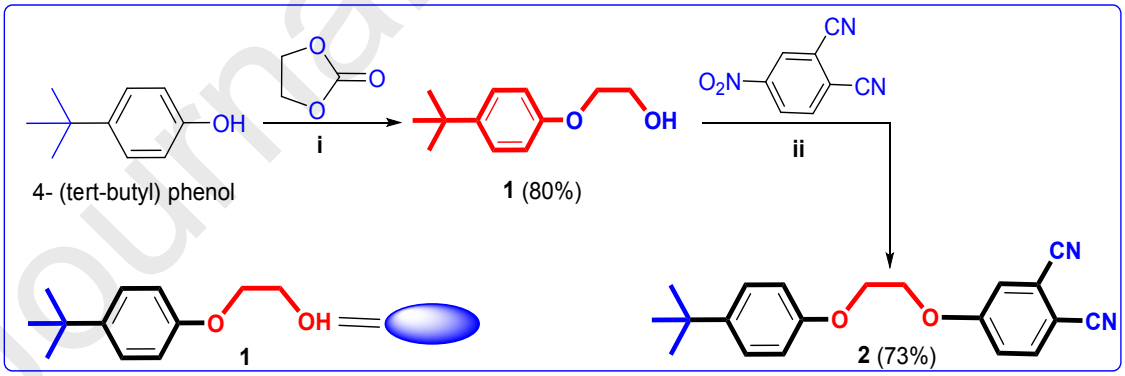

Journal Pre-proofs

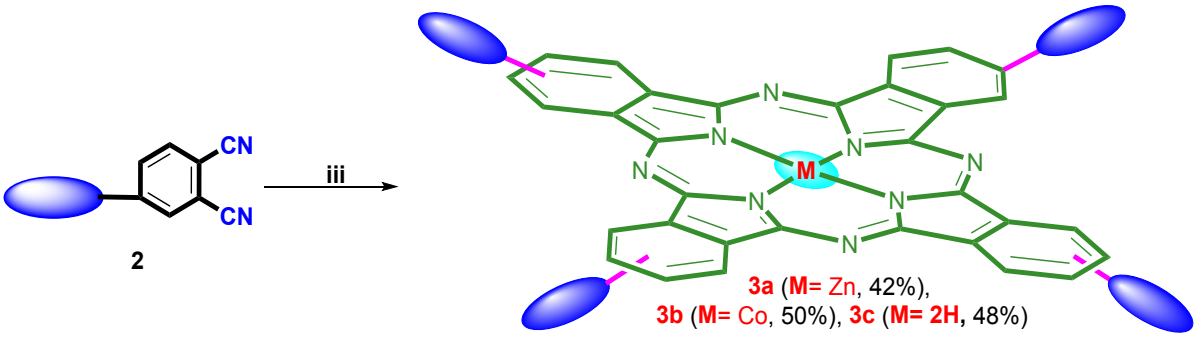

Scheme 1. (**i**) K_2CO_3, DMF, reflux, 24 h; (**ii**) K_2CO_3, DMF, 50 °C; 12 h (**iii**) **3a** $Zn(OAc)_2.2H_2O$, DBU, DMF, 130 °C, 24 h; **3b** $Co(OAc)_2.4H_2O$, DBU, DMF, 130 °C, 24 h; **3c** DBU, DMF, 130 °C, 24 h.

In the UV-vis spectra of the Pcs, the concentration and density of a solvent are interconnected; depending on the increase in concentration for the Q-band absorption, the density will also increase. Moreover, the Q band depends on the environmental conditions and substitution of the Pc macro-ring. Q-band absorption occurs with the transition of the HOMO to the LUMO $\pi \rightarrow \pi^*$ [20]. The UV-vis spectra of the ZnPc, CoPc, and H_2Pc in the experiment are shown in text.

3.2. Aggregation behavior

The electronic spectra of **3a** and **3c** show absorption, emission, and excitation in DMF (Figure 2, Figure 3). The excitation spectra for complex **3a** are different from the absorption and emission spectra in the mentioned solution because of a blue shift giving slight aggregation and a low split at 600-620 nm. However, there is little aggregation in the excitation band relative to the absorption band. According to the excitation spectra, the representation of the unaggregated strong absorption band of **3a** with the low splitting in the Q band is clearer in the fluorescence excitation spectra in DMF (Figure 2). The fluorescence emission Q-band of **3a** is different from the fluorescence absorption and excitation Q-bands (Figure 2), which have red shifted and included aggregation [21,22a]. Pc-**3c**, which does not contain metal, could not detect much different special properties than ZnPc-**3a** containing metal at its center. The absorption, emission, and excitation spectra for **3a** and **3c** in DMF were compared with those in standard ZnPc, and the results are given in Table 1.

Journal Pre-proofs

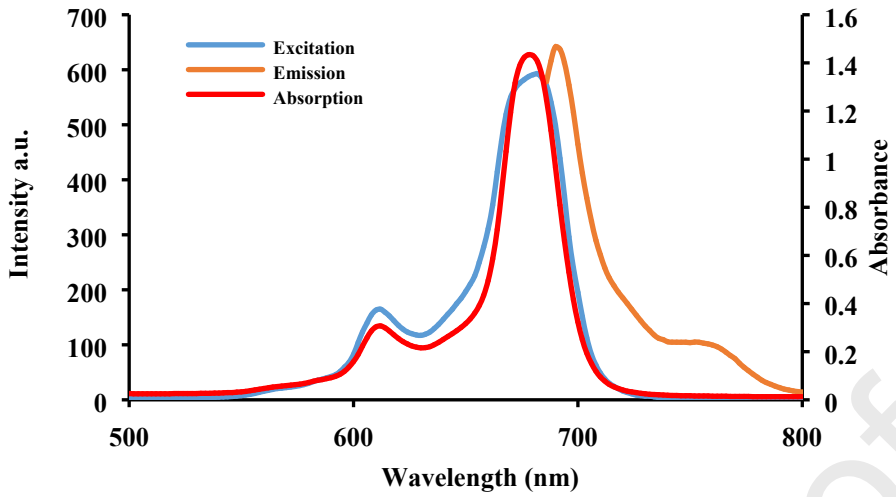

Figure 2. Absorption, excitation, and emission spectra of compound **3a** in DMF. Excitation wavelength 682 nm.

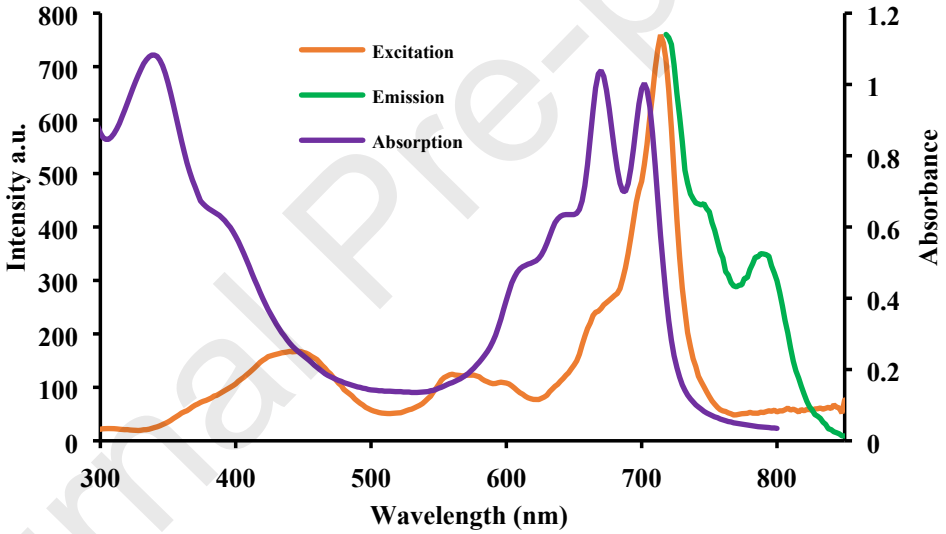

Figure 3. Absorption, excitation, and emission spectra of compound **3c** in DMF. Excitation wavelength 672, 718 nm.

Table 1. Absorption, excitation, and emission spectral data for **3a**, **3c** and standard studied ZnPc.

Compound	Solvent	Q band λ_{max} (nm)	log ε	Excitation λ_{Ex}, (nm)	Emission λ_{Em}, (nm)	Stokes shift (nm)
3a	DMF	680	5.15	682	693	13
3c	DMF	699, 705	4.72, 4.68	672, 718	720	15
ZnPc[a]	DMF	670	5.37	670	676	6

[a] Data from Ref. [22b].

Journal Pre-proofs

For the ZnPc-**3a** in Figure 4, while the B bond region appears between 325 and 375 nm, the Q bond region appears between 660 and 700 nm as a single (narrow) band in different solutions such as DMF, DMSO, and DCM with the same concentration, showing no aggregation except for low splitting at 600-630 nm. This unaggregation is also due to the fact that the tert-butyl substituents in the peripheral position donating electrons to the Pc macro-ring can have high dipole moment [12,13,21].

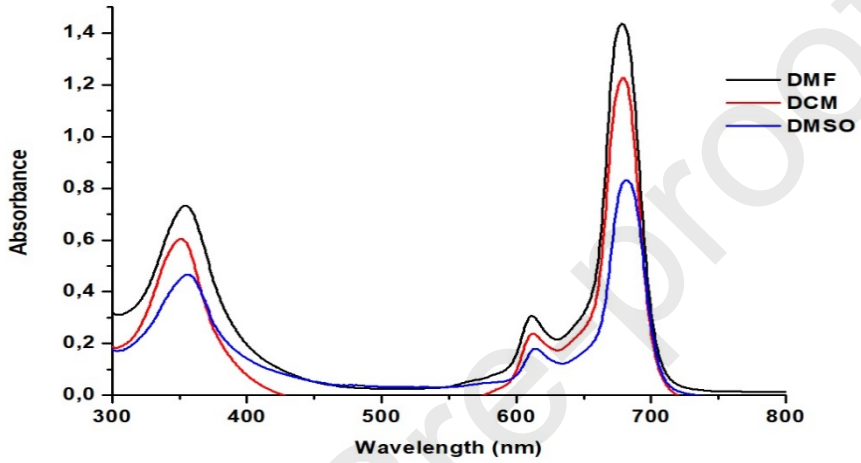

Figure 4. UV-vis of **3a** (1.0×10^{-5} M) in different solutions.

In the CoPc-**3b**, electron-donating tert-butyl groups in a peripheral position donate electron density into the π system and increasing conjugation in the macro-ring, thus causing red shifting and a lower HOMO–LUMO gap [20,21]. In the absorbance-wavelength graph both the B band and Q band cause red shifting in the mentioned solution, showing low aggregation and low splitting at 590-620 nm. (Figure 5.)

Journal Pre-proofs

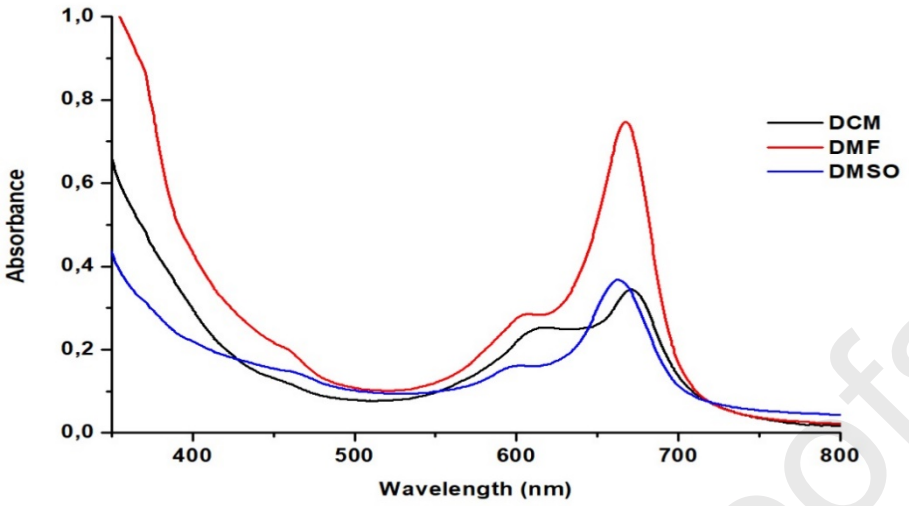

Figure 5. UV-vis of **3b** (1.0×10^{-5} M) in different solutions.

The metal-free Pc LUMO trajectory forms Qx and Qy states with a lower D_{2h} symmetry than planar metallophthalocyanines' D_{4h} symmetry and the Q-band is split into two [23] The B- band and Q-band electronic absorption, which are characteristic for H_2Pc-**3c**, were recorded at a concentration of 1.0×10^{-5} M in the 300-750 nm range. The B band showed strong absorption between 310 and 400 nm, while the Q band showed strong absorption with low aggregation between 610 and 720 nm. Moreover, the small splits seen between 600 and 630 nm belong to the vibration tones of the Q band. (Figure 6.)

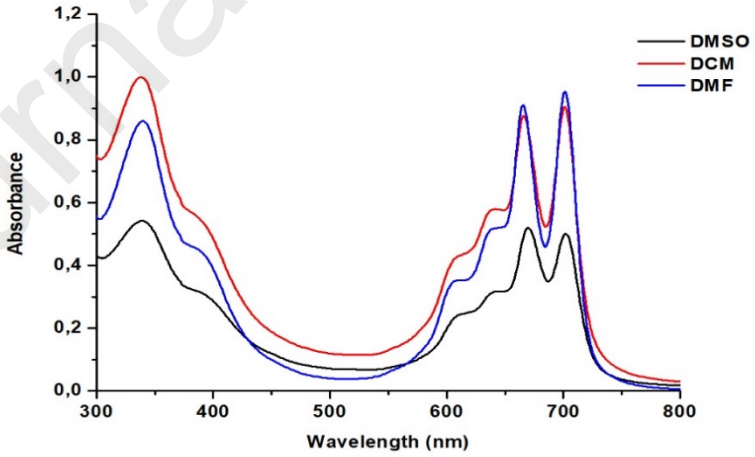

Figure 6. UV-vis of **3c** (1.0×10^{-5} M) in different solutions.

The concentration dependence of complex **3a** in DMF is shown in Figure 7. The intensity of the Q band increases with the increase in solution in different concentrations. In the absorption spectral changes, aggregation also depends on the nature of the solvent, and because of

aggregation there are no new bands [24]. In Figure 7, it is seen that the Lambert–Beer law is obeyed at different concentrations of solvent ranging from 2×10^{-6} to 1×10^{-5} M.

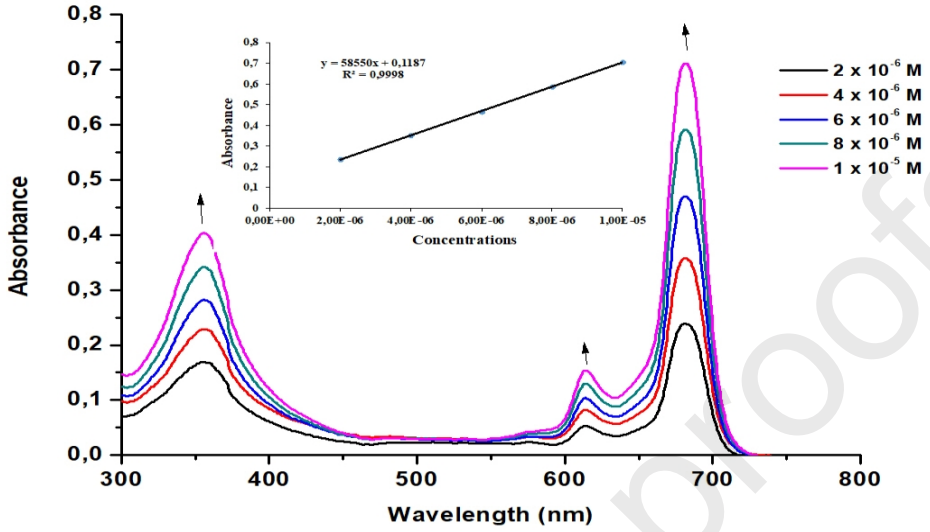

Figure 7. Absorption spectral changes of compound **3a** in DMF at concentrations from 2×10^{-6} to 1×10^{-5} M.

3.3. Photophysical and photochemical parameters

3.3.1. Singlet oxygen quantum yields

The absorbance changes for the determination of singlet oxygen quantum yield were studied in 1.0×10^{-5} M concentration. The experiment was performed in DMF solution in air. After compound **3a** and DPBF were mixed, the results were recorded at regular intervals in a system containing air under light irradiation in the dark. The intensity of the light used was 6.63×10^{15}photons^{-1}cm^{-2}. To avoid the occurrence of side chain reactions the concentration of DPBF was maintained at ~3 × 10^{-5} M. Electronic absorption spectral changes during the investigation of the photodegradation quantum yield were exhibited for compound **3a** and **3c** using DPBF as chemical quencher, compared to the known relative method ZnPc (Figure 8, Table 2) [25-27].

Journal Pre-proofs

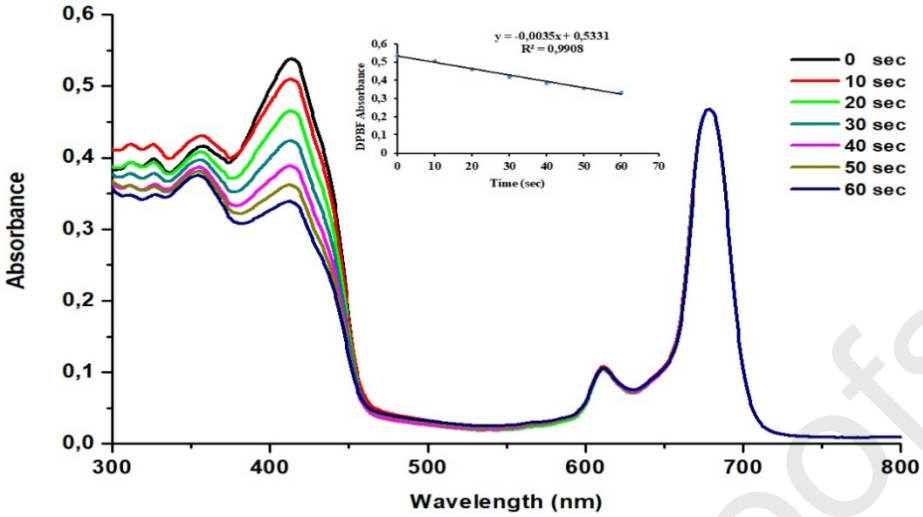

Figure 8. Absorbance changes for the determination of singlet oxygen quantum yield of complex **3a** (1.0×10^{-5} M) in DMF using DPBF as singlet oxygen quencher. (Inset: plot of DPBF absorbance versus time).

Table 2. Photochemical parameters of **3a** and **3c** in DMF.

Compound	Φ_Δ	Φ_d **(x10^{-4})**
3a	0.04	0.45
3c	0.03	0.57
ZnPc[a]	0.56	0.23

[a]Data from Ref.[27]

Equation 3 was used with absorbance changes for the determination of singlet oxygen quantum yield for complex **3a**, and **3c**.

$$\Phi_\Delta = \Phi_\Delta^{Std}\frac{R\ .\ I_{abs}^{Std}}{R^{Std}.I_{abs}}, \qquad (Eq.\ 3)$$

$\boldsymbol{\Phi_\Delta^{Std}}$ in Equal (3) defines the singlet oxygen quantum yield (Φ_Δ) in relation to the standard Zn-Pc method ($\boldsymbol{\Phi_\Delta^{Std}}$=0.56 in DMF). *R* and R^{Std} exhibit DPBF photo-quencher properties in the presence of related samples (**3a** and **3c**). $\boldsymbol{I_{abs}}$ and $\boldsymbol{I_{abs}^{Std}}$ are the rates of light absorption by the samples (ZnPc-**3a** and metal free-**3c**) and the standard, respectively.

3.3.2. Photodegradation studies

Photodegradation, in general, is expressed as the resistance of a molecule to light. Photodegradation quantum yield (Φ_d) can be calculated by examining the change in the

absorption spectrum during light degradation of the compound. The photodegradation of Pcs are observed with a decrease in Q bands during photolysis of the Q-band region at certain time intervals and the photodegradation quantum yield (Φ_d) can be calculated using the slopes of the calibration graphs created at these certain time intervals. After laser radiation, or photolysis, Q bands was decreased over time for compound **3a**. This decrease in Q absorption band was measured between 615-680 nm (Figure 9). Also the same decrease was observed in Q bands absorption between 699-705 nm for compound **3c**. All results are exhibited in Table 2. A light intensity of 3.26×10^{16} photons s^{-1} cm^{-2} was employed for Φ_d determinations.

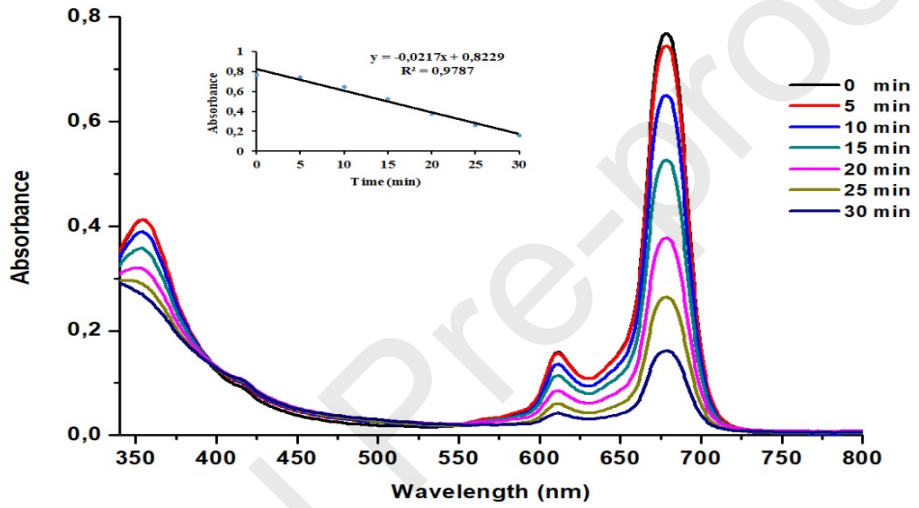

Figure 9. Electronic absorption spectral changes during the investigation of the photodegradation quantum yield of compound **3a** (1.0×10^{-5} M). (Inset: plot of absorbance versus time).

Absorption spectral changes during the investigation of photodegradation quantum yield (Φ_d) for compound **3a** and **3c** were calculated by Equal 4 [28,29].

$$\Phi_d = \frac{(C_0 - C_t).\,V.\,N_A}{I_{abs}\,.\,S.\,t}, \qquad (Eq.\,4)$$

Here C_0 is the concentration before irradiation, C_t is the concentration after irradiation, V is volume, N_A is the Avogadro constant, S is irradiated cell area, t is irradiation time, and I_{abs} is the overlap integral of the radiation source light intensity [30].

3.3.3. Fluorescence quenching studies of 1,4-benzoquinone (BQ)

The fluorescence quenching assays for the complex **3a** and **3c** were performed by adding benzoquinone (BQ) at different concentrations of saturated solutions of MPc, obeyed the Stern–Volmer equation and kinetics for calculation the change in fluorescence intensity [31]. Fluorescence emission reduction of compound **3a** by adding BQ at different concentrations (0, 0.008, 0.016, 0.024, 0.032, and 0.040 mol dm^{-3}) in DMF is shown in Figure 10. Because of the high electron affinity of quinones and their good participation in electron transfer processes, the lowest excited state energy for them is greater than the excited single state energy of MPc complexes [32-34]. Therefore, it is unlikely that energy transfer from exciting MPc to BQ will occur and MPc are known to be readily reduced. Accordingly, fluorescence MPc quenched by BQ occurs through electron transfer of excited state from MPc to BQ [35]. The Stern-Volmer constant value (Figure 10) were calculated in DMF (Ksv = 60.1 M^{-1} for **3a**, Ksv = 13.4 M^{-1} for **3c**), on the slope plot graph against BQ concentration [32]. According to Stern-Volmer constant, the Ksv value of ZnPc complex **3a** was higher than the standard Sdt-ZnPc, whereas the Ksv value of H_2Pc complex **3c** was showed lower than the Sdt-ZnPc (Std-ZnPc Ksv = 57.60 M^{-1} in DMF).

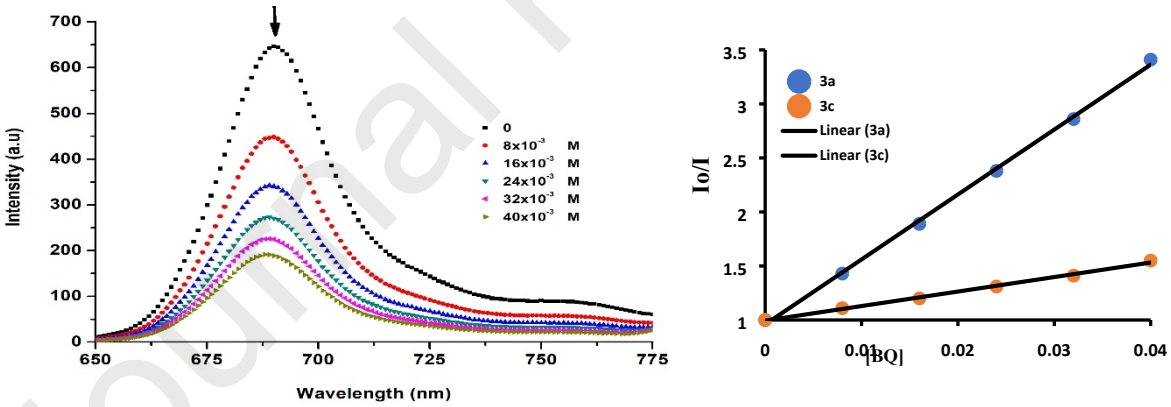

Figure 10. (Left) Fluorescence emission spectral changes of **3a** (1.0×10^{-5} M) on addition of different concentrations of BQ in DMF. (Right) Stern-Volmer plot for BQ quenching of substituted phthalocyanines (ZnPc **3a** and H_2Pc **3c**) in DMF. [BQ] = 0, 0.008, 0.016, 0.024, 0.032, 0.040 M.

$$I_0/I = 1 + K_{SV}[BQ]. \quad (Eq.\ 5)$$

The fluorescence intensities are shown by I_0 and I, which are the fluorescence intensities of fluorophore in the absence and presence of quencher, respectively. The concentration of

quencher is indicated by [BQ]. K_{SV} is the Stern–Volmer constant [31]. The ratios of I_0/I were calculated and plotted against [BQ] according to Equal 5, and K_{SV} was determined from the slope [36].

3.3.4. Determination of Binding of Pc Compounds with CT-DNA

The use of UV-vis spectroscopy to determine the mode of binding of a compound to DNA is a useful in vitro instrumental technique that gives information about band position in the spectrum for the molecular interaction based on shifting [18,37,38]. Shifting indicates the strength of the interaction between DNA and Pcs, in which in these aqueous solutions of Pcs cause aggregation and this aggregation can sometimes be severe. In some cases, aggregation can greatly reduce the Q band absorption [39]. The interaction of Pcs with DNA was investigated by electronic absorption spectroscopy in terms of how the Pcs change the UV-absorption band in the presence of DNA, and the interaction between the double bonded DNA with the Pcs during the titration of the DNA [18, 38,40]. The UV spectrum of compound **3a** was recorded at constant (7.5 µM) concentration before and after the stepwise increase in DNA concentration (0, 5, 10, 15, 20, 25 µM) for DNA binding studies. In the event of intercalation a strong stacking interaction occurs between compounds and the base pairs of DNA, and with this strong stacking interaction the binding of an intercalative compound to DNA causes hypochromism (decrease in absorption intensity) and significant bathochromism (red shift at wavelength) in the absorption spectrum [38-40]. Compound **3a** was studied in different DNA concentrations and the results are shown in Figure 11.

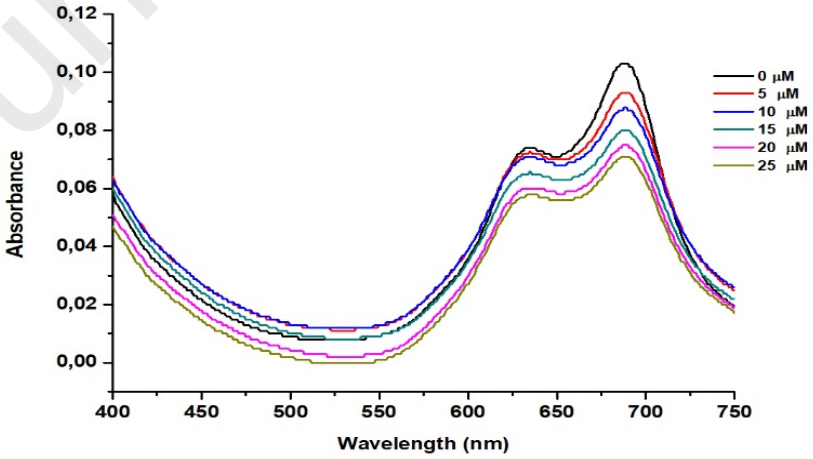

Figure 11 UV-vis absorption spectra of **3a** upon increasing amounts of CT-DNA (0, 5, 10, 15, 20, 25 µM) (from top to bottom).

The increase in DNA concentration between 400 and 750 nm exhibited for compound **3a** in the optimal absorption condition remained stable, but the spectral data exhibited hypochromism (decrease in absorbance value) upon the addition of CT-DNA. Hypochromism is the spectral feature of dsDNA showing changes in the double helix structure, and which is an indicator of electrostatic or intercalation-like interactions between dsDNA and compounds, and also must be accompanied by a red shift (bathochromic shift) for an intercalative interaction [41].
In electronic absorption titration, batchromism (redshift), hypochromite and isosbestic point, because of π-π* strong interaction between tert-butyl substituent and DNA bases are compatible with intercalation [42]. The stacking interaction of the Pcs and DNA base pairs, are affected by binding electron donating tert-butyl substituent on the Pcs ring, and this electron-donating substituents are also exhibit the interaction of the aromatic π system on the metal atom in the cavity. The stacking interaction between aromatic π system on the metal and electron donating system for compound **3a** caused 31% bathochromism (Figure 11). Also, the hypochromic effect was observed without any red shifting, non-intercalative binding mode of **3a** with CT-DNA.

3.3.5. DPPH Radical Scavenging Assay

The basis of this method is the reduction of DPPH with a synthesized molecule gives a strong violet color during reduction. This reduction causes the color of the radical to change from violet to yellow during reduction at quantifiable levels using a spectrophotometer in 517 nm [43]. The antioxidant capacity of synthesized compounds is detected by DPPH radical scavenging assay[18, 40,44]. In the present study, Pcs were synthesized that have the ability to scavenge DPPH radicals. The experiment was carried out according to a previously described procedure[17]. After the preparation of the Pc stock solutions in DMSO, DPPH solution in MeOH was mixed and then the stock solution was used at different concentrations ranging from 25 to 50 mL in the experiment. DMSO as a control was used in instead of the tested Pcs. The DPPH radical cleaning capacity of the Pcs is exhibited in Table 3 against gallic acid in different concentrations. The observation of the antioxidant capacity for compound **3b** (32.81 ± 0.40% for 100 μM concentration) may have higher DPPH activity than compounds **3a** (14.55 ± 0.19%) and **3c** (22.74 ± 0.15% for 100 μM concentration), since it has redox active metal atoms, and the results showed that the antioxidant capacities for Pcs (**3a**, **3b**, and **3c**) , are not as effective as gallic acid, when their DPPH radical cleaning capacity calculated according to the

concentration range (14.57 ± 0.31%, 22.58 ± 0.35%, 30.63 ± 0.32%, 32.81 ± 0.40%) (Table 3, Figure 12).

As a result, it is though that the effect of the electron donating system (tert-butyl groups bearing pheripheral position) give rise to the change electron density around center metal atom in the cavity of MPc and influenced by resonance of localized π electron system. The DPPH behavior is directly relative to this resonance of localized π electron system, and metal atom that entering to the cavity of MPc have directly affected by the π electron system and also, this resonance localized π electron system, change the result of DPPH or redox activity of center metal atoms. So, gallic acid showed more DPPH free radical scavenging activity than the tested compounds (**3a**, **3b**, and **3c**).

Table 3. Radical-scavenging activity on DPPH radicals (%) of the phthalocyanines.

µM[a]	3a	3b	3c	Gallic Acid[c]
25	3.02 ± 0.09 [b]	14.57 ± 0.31 [b]	5.55 ± 0.11 [b]	68.88 ± 0.40 [b]
50	7.79 ± 0.12 [b]	22.58 ± 0.35 [b]	8.46 ± 0.11 [b]	81.53 ± 0.42 [b]
75	9.39 ± 0.15 [b]	30.63 ± 0.32 [b]	15.52 ± 0.19 [b]	87.71 ± 038 [b]
100	14.55 ± 0.19 [b]	32.81 ± 0.40 [b]	22.74 ± 0.15 [b]	90.58 ± 0.50 [b]

[a] Four experiments were performed for all compounds in each experiment in triplicate.
[b] Mean values ± SD are shown for triplicate experiments.
[c] Reference compound.

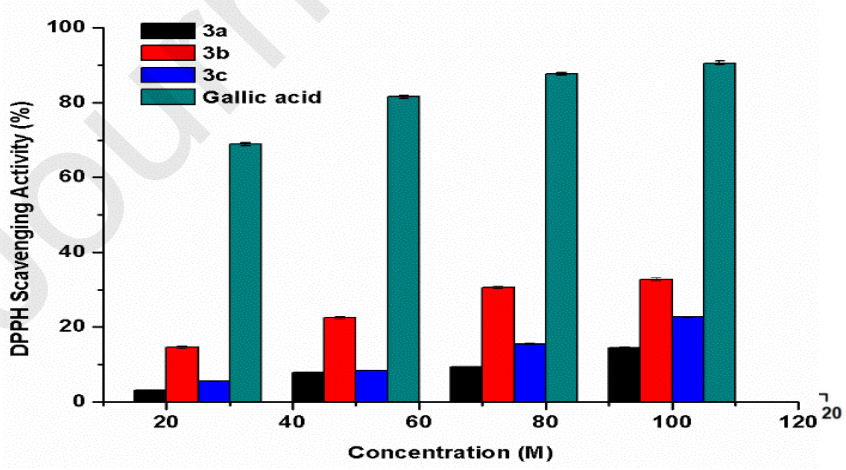

Figure 12. Scavenging ability of compounds

3.3.6. Metal Ions Chelating Effects Assay

Journal Pre-proofs

Fe^{+2} is a feasible therapeutic approach to prevent radicals in Fe^{+2} chelation metabolism, as single electrons are capable of acting from peroxides that permit the formation of alkoxy radicals [18,45]. Divalent iron chelates ferrozine iron quantitatively by forming a colored complex. The presence of another chelator may hinder complex formation, which leads to a decrease in color, and the measurement of this color reduction helps to predict the chelating capacities of the chelator candidates [45]. The Pcs metal chelating activity was conducted at 25, 50, 75, and 100 metal concentrations by using 1 mM stock solutions in DMSO. The chelating (%) activity of ions and complexes (**3a**, **3b**, and **3c**) shows that chelating activity is increased relative to the increasing concentrations used (Table 4). At the end of the experiment **3c** was found to be good chelator for Fe^{+2} chelating capacity, as 26.96 ± 0.39%, up to 100 µM concentration. The other complexes (**3a** and **3b**) showed lower iron-containing ion chelating properties compared to EDTA, The results showing that they have high metal chelating properties at the different concentrations mentioned for Pcs are reported in the Table 4 [18]. According to the results in table 4, the tert-butyl substituent bearing onto peripheral position of the Pcs were positively affected the cavity. So, it can be say that the Pc gained ferrous ion-ferrozine complex formation (FIC ability) owing to involving metal atoms in the inner core and have affected the lower values of Pcs and gained high antioxidant properties. Also, the ferrious chelating activity and concentration of compound was exhibited in the plot in Fig. 13.

Table 4. Ferrous ions chelating activity (%) of the phthalocyanines.

µM[a]	3a	3b	3c	EDTA[c]
25	2.25 ± 0.11 [b]	10.63 ± 0.22 [b]	5.87 ± 0.25 [b]	15.65 ± 0.15 [b]
50	5.41 ± 0.05 [b]	16.52 ± 0.09 [b]	11.52 ± 0.37 [b]	51.42 ± 0.18 [b]
75	8.63 ± 0.07 [b]	21.74 ± 0.76 [b]	17.63 ± 0.24 [b]	82.31 ± 0.08 [b]
100	11.62 ± 0.06 [b]	24.96 ± 0.51 [b]	26.96 ± 0.39 [b]	96.85 ± 0.21 [b]

[a] Four experiments were performed for all compounds in each experiment in triplicate.
[b] Mean values ± SD are shown for triplicate experiments.
[c] Reference compound.

Journal Pre-proofs

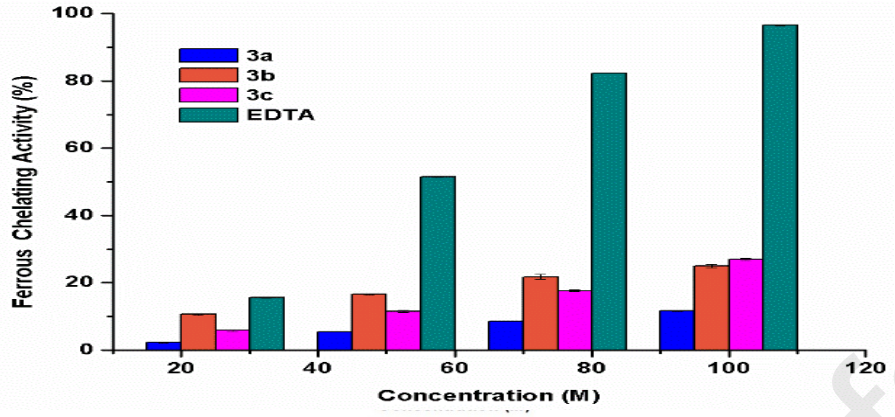

Figure 13. Chelating ability of the compounds.

4. Conclusion

Three new phthalocyanines were prepared. For the synthesis of MPcs [M = Zn (**3a**) and M = Co (**3b**)], the 4-(2-(4-(tert butyl)phenoxy)ethoxy) phthalonitrile **2** was reacted with metal salts ($Zn(OAc)_2.2H_2O$, $Co(OAc)_2.4H_2O$) in the presence of a catalyst (DBU). For the synthesis of metal-free phthalocyanine [H_2Pc (**3c)**], without using a metal salt as mentioned, the 4-(2-(4-(tert butyl)phenoxy)ethoxy) phthalonitrile was reacted in the same condition. The photophysical and photochemical parameters of the resulting molecules (**3a**, **3b**, and **3c**) were determined. The photodegradation quantum yield (Φ_d) of **3a** and **3c** are higher than those of standard ZnPc (Tablo 2). In the photochemical study, the singlet oxygen production and photo degradation of **3a** were measured. Photodegradation showed an increase parallel to the literature. Therefore, **3a** has the potential to be used in photodynamic therapy.

The DNA binding mode of Pcs with CT-DNA was analyzed quantitatively. K_b values of **3a** estimated from the Wolfe–Shimmer equation were 5.2 (± 0.52) 10^3 M^{-1}. The binding constant of **3a** is lower than that of ethidium bromide, a known DNA intercalator (K_b = 1.23 ± 0.07 × 10^5). These results suggest the existence of non-intercalative interactions between the synthesized Pcs and CT-DNA.

When the results obtained in this study are compared with those of other studies done with Pcs, it is possible to see compounds with similar K_b values [15,40]. Moreover, these higher K_b values were reported for a zinc Pc [40] and manganese and copper Pcs [29]. In addition, the Pc **3b** is a good chelator for Fe^{+2} chelating capacity with 24.96 ± 0.51% up to 100 µM concentration. The

other Pcs (**3a** and **3c**) show low iron-containing ion chelating properties compared to EDTA. The DPPH radical cleaning capacity of Pcs was shown against gallic acid in different concentrations. The observation of the highest antioxidant capacity exhibited for all Pcs (**3a**, **3b**, and **3c**) showed they were not as effective as gallic acid when their DPPH radical cleaning capacity was calculated according to the concentration range (14.57 ± 0.31%, 22.58 ± 0.35%, 30.63 ± 0.32%, 32.81 ± 0.40%).

CONFLICT OF INTEREST

The authors confirm that this article content has no conflict of interest.

ACKNOWLEDGEMENT

This study was supported by The Scientific and Technological Research Council of Turkey (TÜBİTAK, project no: 115Z446 and 217Z043).

REFERENCES

[1] C.C. Leznoff, A.B.P. Lever, Advanced Materials. 5 (**1993)** 942–943.

[2] M. Hanack, M. Lang, Advanced Materials. 6 (**1994)** 819–833.

[3] N.B. Mckeown, English, Book, Cambridge, U.K., New York, Cambridge University Press. (**1998)** 193.

[4] S.V. Kudrevich, M.G. Galpern, J.E. Van Lier, Synthesis. (**1994)** 779–781.

[5] F. Mitzel, S. Fitzgerald, A. Beeby, R. Faust, Chemical Communications. 24 (**2001)** 2596–2597.

[6] E.M. Maya, E.M. García Frutos, P. Vázquez, T. Torres, G. Martín, G. Rojo, J. Zyss, The Journal of Physical Chemistry A. 107 (**2003)** 2110–2117.

[7] K. Ban, K. Nishizawa, K. Ohta, H. Shirai, Journal of Materials Chemistry **(2000)** 1083–1090.

[8] D. Wöhrle, Advanced Materials. 5(12) (**1993)** 942–943.

[9] X. Du, G. Du, C. Ma, D. Tian, X. Hou, Y. Chang, H. Yu, Synthesis. (**2005)** 741–748.

[10] K. Sakamoto, E. Ohno-Okumura, Materials. 2 **(2009)**, 1127-1179.

[11] M.S. Agirgtas, O. Bekaroglu, J. Porphyrins Phthalocyanines. **(2001)** 717.

Journal Pre-proofs

[12] C.C. Leznoff, S.M. Marcuccio, S. Greenberg, A.B.P. Lever, K.B. Tomer, Canadian Journal of Chemistry. (**1985)** 623–631.

[13] W. Eberhardt, M. Hanack, Synthesis. (**1997)** 95–100.

[14] J.V. Bakboord, M.J. Cook, E. Hamuryudan, Journal of Porphyrins and Phthalocyanines. **(2000)** 510–517.

[15] B. Nilsson, J. Tejbrant, B. Pelcman, E. Ringberg, M. Thor, J. Nilsson, M. Jönsson, United States Patent. (**2006)** US 7,071,180 B2.

[16] A. Wolfe, G.H. Shimer, T. Meehan, Biochemistry. **(1987)** 6392–6396.

[17] P. Carter, Analytical Biochemistry. (**1971)** 450–458.

[18] A. Özel, B. Barut, Ü. Demirbaş, Z. Biyiklioglu, Journal of Photochemistry and Photobiology B, Biology. **(2016)** 32–38.

[19] M.S. Bloıs, Nature. (**1958)** 1199–1200.

[20] D.K. Modibane, T. Nyokong, Polyhedron. **(2008)** 1102–1110.

[21] M.J. Stillman, T. Nyokong, C.C. Leznoff, New York, Chapter 1 (**1989)**.

[22] a) W. Freyer, S. Mueller, K. Teuchner, Journal of Photochemistry and Photobiology A: Chemistry. 163 **(2004)** 231–240. b) M. Çamur, M. Durmuş, M. Bulut, Polyhedron. (**2012)** 92–103.

[23] D. Wöhrle, M. Eskes, K. Shigehara, A. Yamada, Synthesis. (**1993)** 194–196.

[24] H. Engelkamp, R.J.M. Nolte, Journal of Porphyrins and Phthalocyanines. (**2000)** 454–459.

[25] I. Seotsanyana Mokhosi, N. Kuznetsova, T. Nyokong, J. Photochem. Photobiol. A: Chem. 140 **(2001)** 215-222.

[26] M.D. Maree, N. Kuznetsova, T. Nyokong, J.Photochem. Photobiol. A: Chem. 140 (**2001)** 117-125.

[27] N.A. Kuznetsova, N.S. Gretsova, E.A. Kalmykova, E.A. Makarova, S. Daskevich, V.M. Negrimovskii, O.L. Kaliya, E. A. Luk'yanets, Russ. J. Gen. Chem. **(2000)** 133-140.

[28] R. Bayrak, H.T. Akçay, M. Pişkin, M. Durmuş, I. Değirmencioğlu, Dyes and Pigments. 95 **(2012)** 330–337.

[29] T. Nyokong, Coordination Chemistry Reviews. 251 **(2007)** 1707–1722.

[30] A. Ogunsipe, T. Nyokong, Journal of Photochemistry and Photobiology A: Chemistry. 173 **(2005)** 211–220.

Journal Pre-proofs

[31] A.A. Esenpınar, M. Durmus, M. Bulut, Spectrochimica Acta Part A. 79 (**2011)** 608–617.

[32] Y.Zorlu, F.Dumoulin, M.Durmuş, and V.Ahsen, Tetrahedron. 66 (**2011)** 3248-3258.

[33] A. Ogunsipe and T. Nyokong, Journal of Porphyrins and Phthalocyanines. 9 (**2005)** 21–129.

[34] J. R. Darwent, I. McCubbin, and D. Phillips, Journal of the Chemical Society, Faraday Transactions 2. 78 (**1982)** 347–357.

[35] M. Idowu, T. Nyokong, Journal of Photochemistry and Photobiology A. 204 (**2009)** 63–68.

[36] G. Gümrükçü, G.K. Karaoğlan, A. Erdoğmuş, A. Gül, U. Avcıata, Journal of Chemistry. **(2014)** 1–11.

[37] T. Keleş, B. Barut, Z. Biyiklioglu, A. Özel, Dyes and Pigments. 139 (**2017)** 575–586.

[38] A.M. Zhang, J. Huang, X.C. Weng, J.X. Li, L.G. Ren, Z.B. Song, Y. Zhou, Chemistry Biodiversity. (**2007)** 215–223.

[39] V. Çakır, D. Çakır, M. Göksel, M. Durmuş, Z. Bıyıklıoğlu, H. Kantekin, Journal of Photochemistry and Photobiology A: Chemistry. 299 (**2015)** 138–151.

[40] G.K. Kantar, Ö. Faiz, O. Şahin, S. Şaşmaz, Journal of Chemical Sciences. 129 **(2017)** 1247–1256.

[41] C. Uslan, B. Ş. Sesalan, Inorganica Chimica Acta. 394 **(2013)** 353–362.

[42] G. Ayyannan, M. Mohanraj, G. Raja, N. Bhuvanesh, R. Nandhakumar, C. Jayabalakrishnan, J Photochem Photobiol B Biol 2016;163: 1-13.

[43] K. Pavithra, S. Vadivukkarasi, Food Science and Human Wellness. (**2015)** 42–46.

[44] S. Kauthale, S. Tekale, M. Damale, J. Sangshetti, R. Pawar, Bioorganic Medicinal Chemistry Letters. (**2017)** 3891–3896.

[45] J.P. Adjimani, P. Asare, Toxicology Reports. **(2015)** 721–728.

Journal Pre-proofs

Photophysical, photochemical and DNA binding studies of prepared phthalocyanines

Arif Baran*, Sumeyye Çol, Emel Karakılıç , Furkan Özen

Sakarya University, Faculty of Arts and Sciences, Chemistry Department, 54187, Sakarya, Turkey

abaran@sakarya.edu.tr

Graphical Abstract

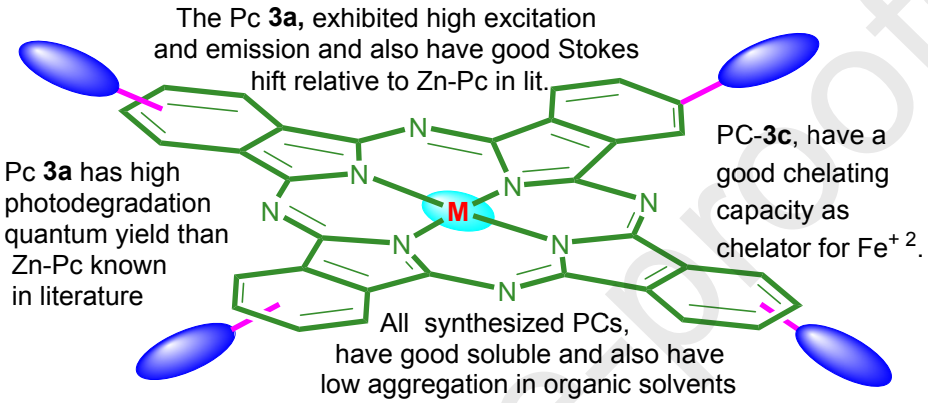

Photophysical, photochemical and DNA binding studies of prepared phthalocyanines

Arif Baran*, Sumeyye Çol, Emel Karakılıç , Furkan Özen

[1]*Sakarya University, Faculty of Arts and Sciences, Chemistry Department, 54187, Sakarya, Turkey*

abaran@sakarya.edu.tr

Highlights

- Three new and efficient synthesis of phthalocyanine were performed.
- The soluble and aggregation behavior of new Pcs were examined.

Journal Pre-proofs

- DNA binding, metal chelating, and DPPH radical scavenging activity were investigated.

Figures

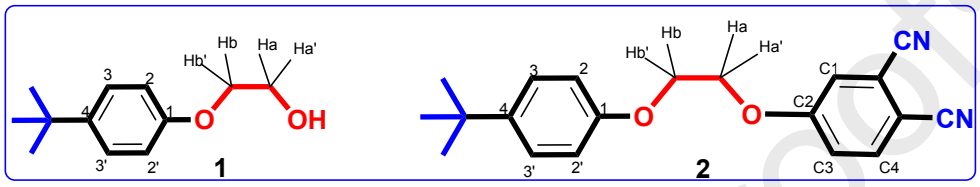

Figure 1. 2-(4-(tert-butyl)phenoxy)ethan-1-ol (**1**) and 4-(2-(4-(tert-butyl)phenoxy)ethoxy) phthalonitrile (**2**)

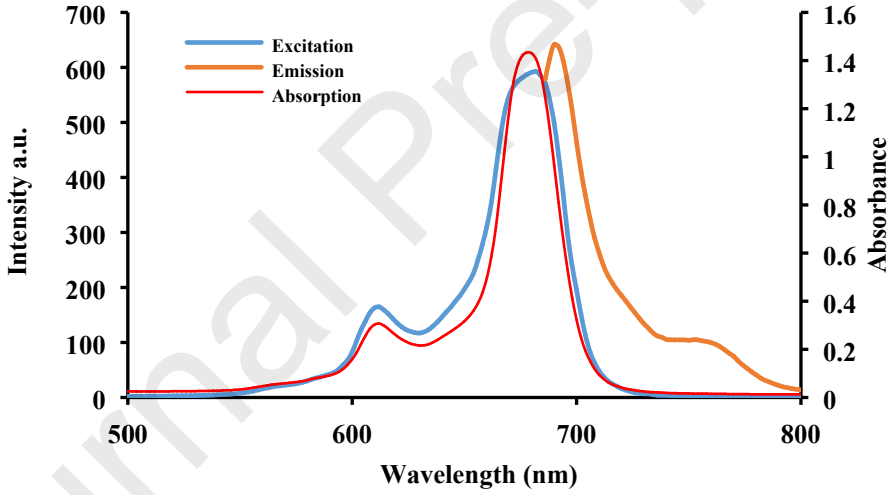

Figure 2. Absorption, excitation, and emission spectra of compound **3a** in DMF. Excitation wavelength 682 nm.

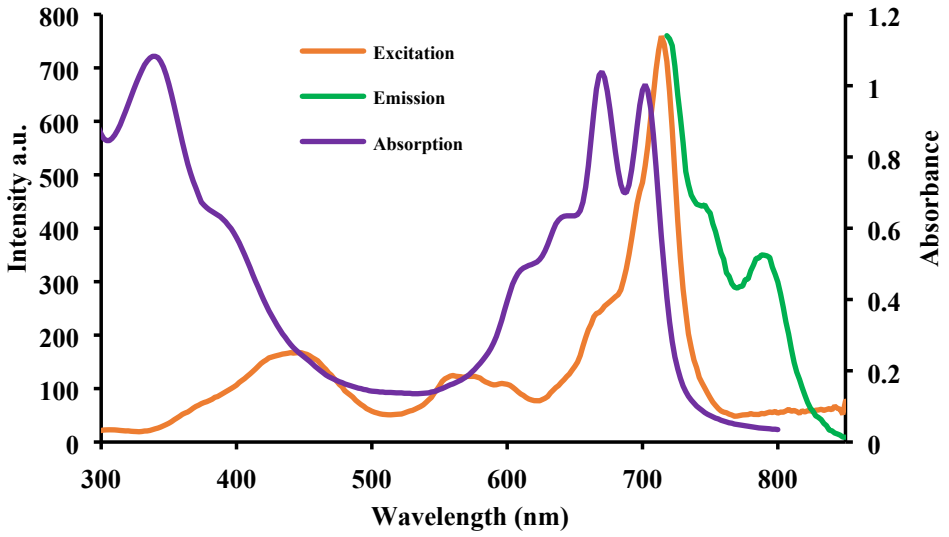

Journal Pre-proofs

Figure 3. Absorption, excitation, and emission spectra of compound **3c** in DMF. Excitation wavelength 672, 718 nm.

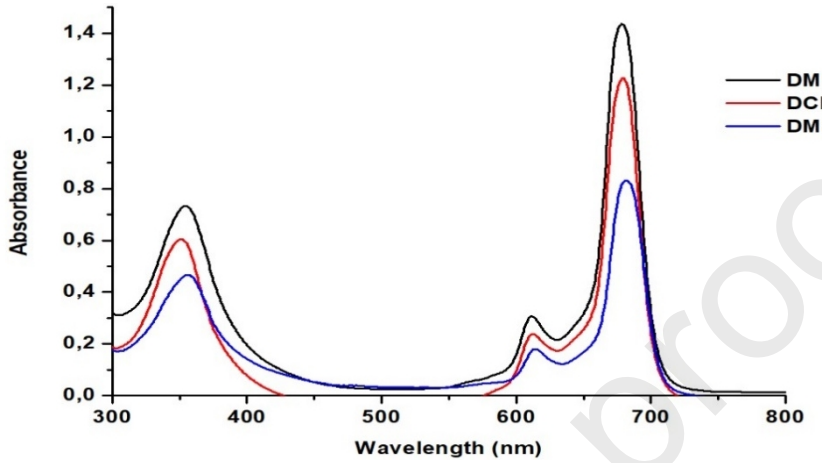

Figure 4. UV-vis of **3a** (1.0×10^{-5} M) in different solutions.

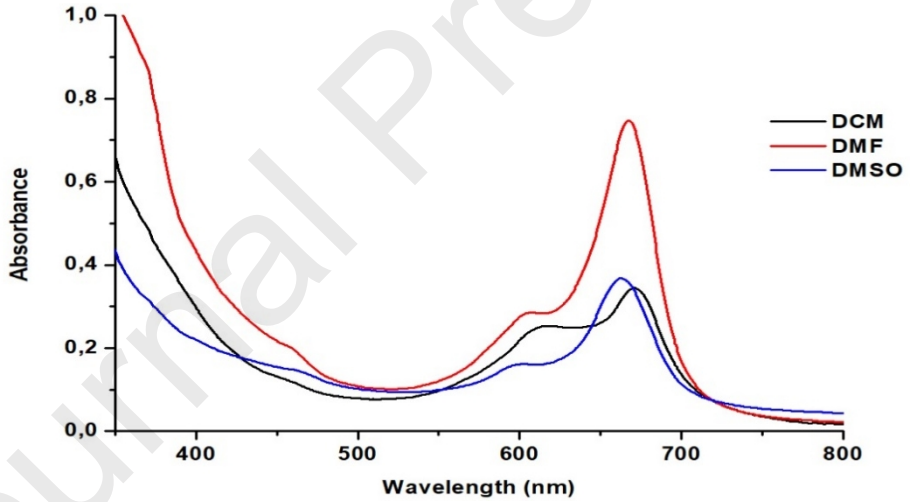

Figure 5. UV-vis of **3b** (1.0×10^{-5} M) in different solutions.

Journal Pre-proofs

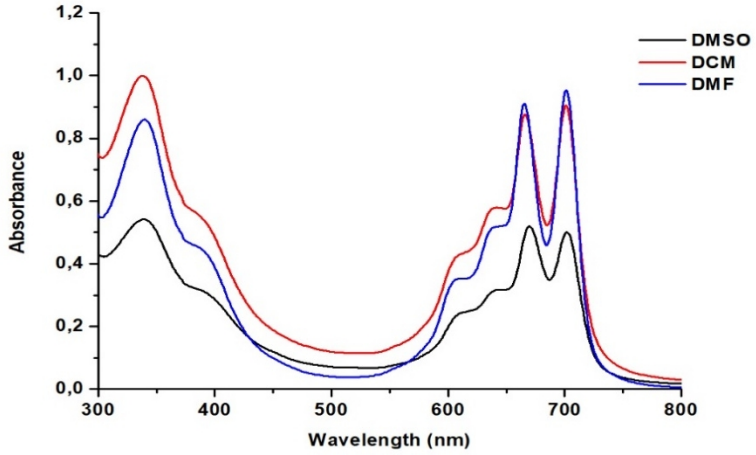

Figure 6. UV-vis of **3c** (1.0×10^{-5} M) in different solutions.

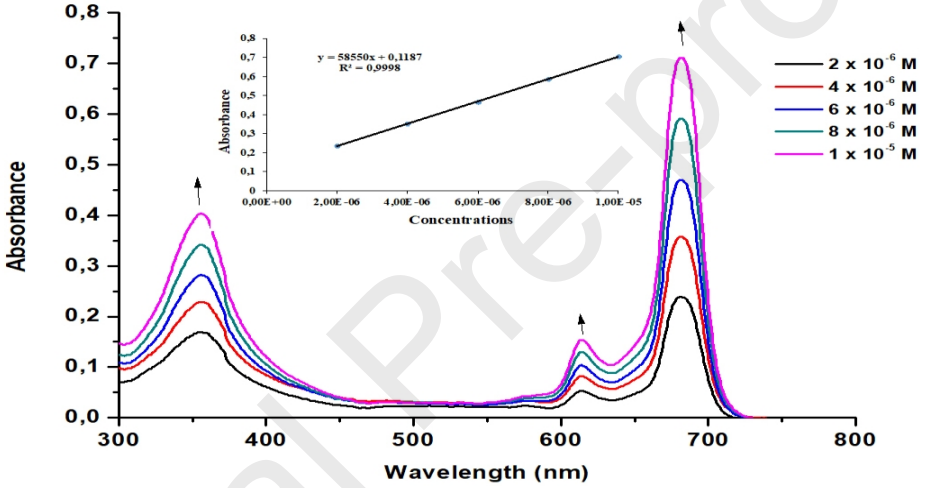

Figure 7. Absorption spectral changes of compound **3a** in DMF at concentrations from 2×10^{-6} to 1×10^{-5} M.

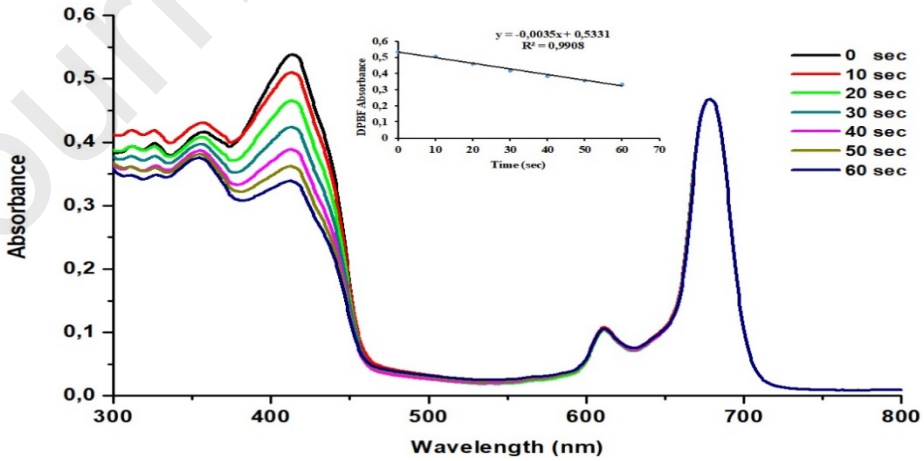

Figure 8. Absorbance changes for the determination of singlet oxygen quantum yield of complex **3a** (1.0×10^{-5} M) in DMF using DPBF as singlet oxygen quencher. (Inset: plot of DPBF absorbance versus time).

Journal Pre-proofs

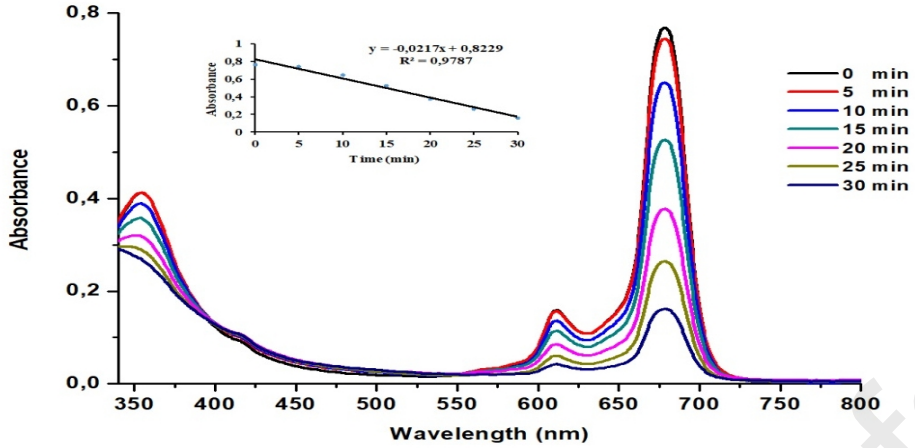

Figure 9. Electronic absorption spectral changes during the investigation of the photodegradation quantum yield of compound **3a** (1.0×10^{-5} M). (Inset: plot of absorbance versus time).

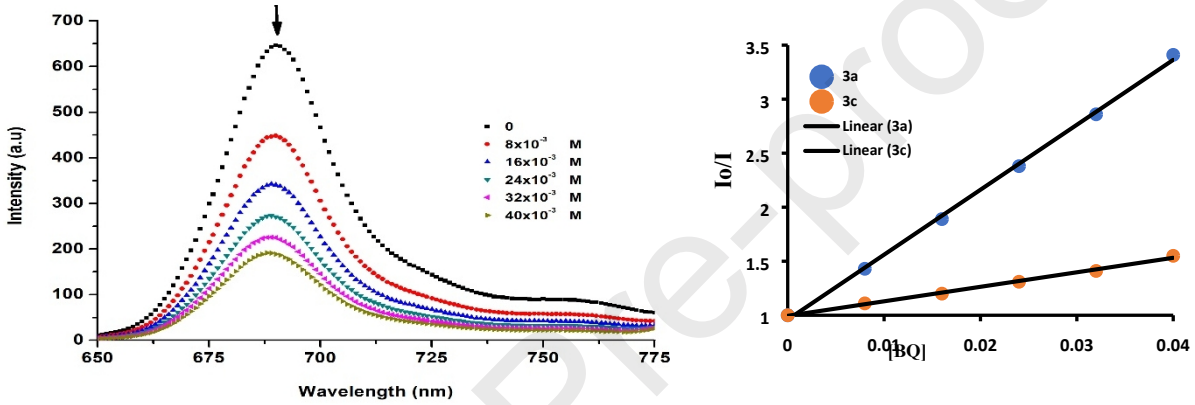

Figure 10. (Left) Fluorescence emission spectral changes of **3a** (1.0×10^{-5} M) on addition of different concentrations of BQ in DMF. (Right) Stern-Volmer plot for BQ quenching of substituted phthalocyanines (ZnPc **3a** and H_2Pc **3c**) in DMF. [BQ] = 0, 0.008, 0.016, 0.024, 0.032, 0.040 M.

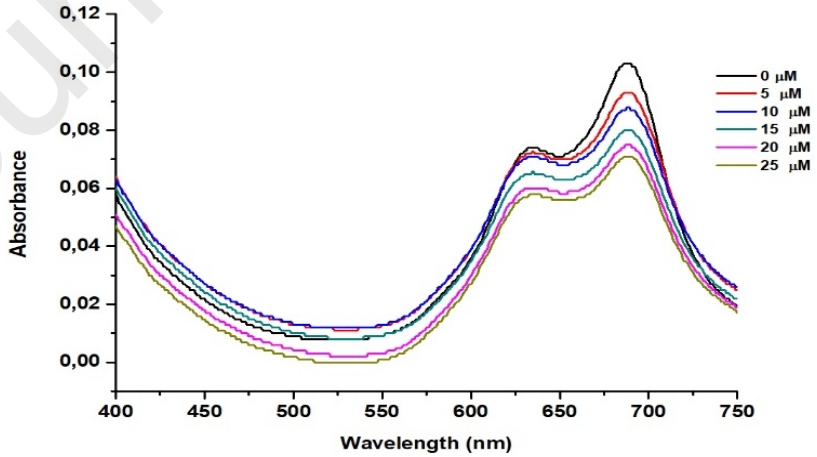

Figure 11 UV-vis absorption spectra of **3a** upon increasing amounts of CT-DNA (0, 5, 10, 15, 20, 25 µM) (from top to bottom).

Journal Pre-proofs

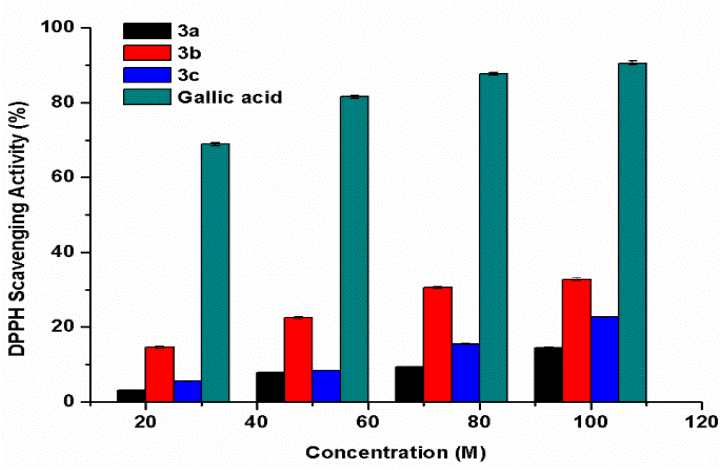

Figure 12. Scavenging ability of compounds

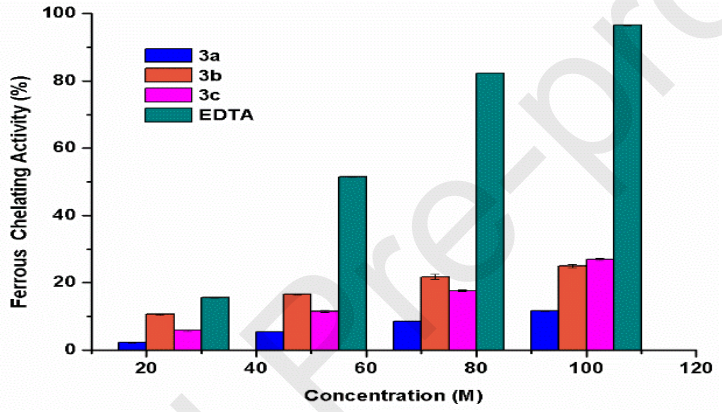

Figure 13. Chelating ability of the compounds.

Tables and Schemes

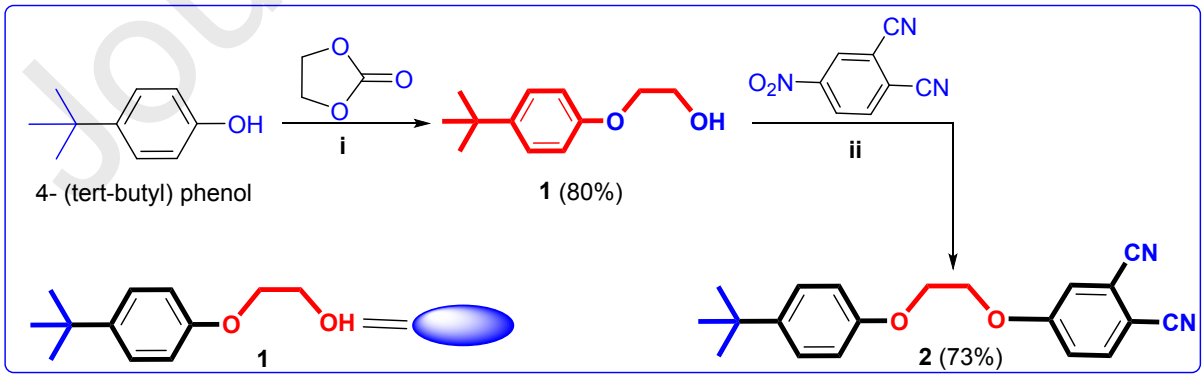

Journal Pre-proofs

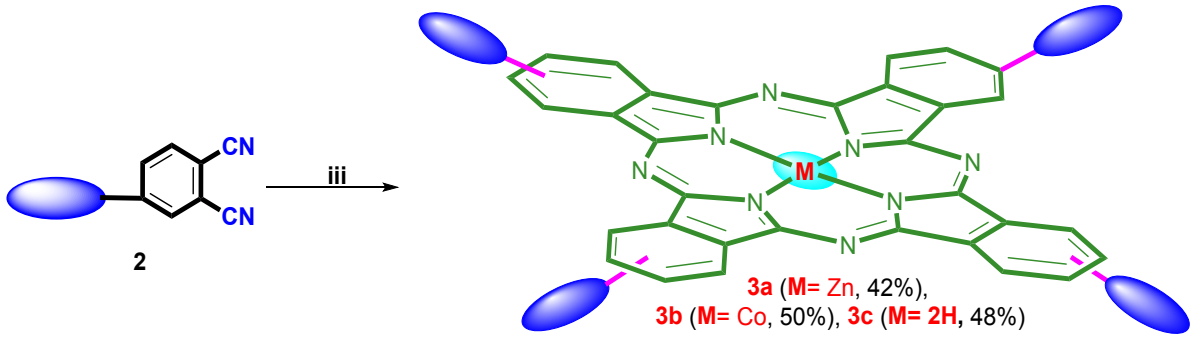

Scheme 1. (**i**) K_2CO_3, DMF, reflux, 24 h; (**ii**) K_2CO_3, DMF, 50 °C; 12 h (**iii**) **3a** $Zn(OAc)_2.2H_2O$, DBU, DMF, 130 °C, 24 h; **3b** $Co(OAc)_2.4H_2O$, DBU, DMF, 130 °C, 24 h; **3c** DBU, DMF, 130 °C, 24 h.

Table 1. Absorption, excitation, and emission spectral data for **3a**, **3c** and standard studied ZnPc.

Compound	Solvent	Q band λ_{max} (nm)	log ε	Excitation λ_{Ex}, (nm)	Emission λ_{Em}, (nm)	Stokes shift (nm)
3a	DMF	680	5.15	682	693	13
3c	DMF	699, 705	4.72, 4.68	672, 718	720	15
ZnPc[a]	DMF	670	5.37	670	676	6

[a] Data from Ref. [22b].

Table 2. Photochemical parameters of **3a** and **3c** in DMF.

Compound	**Φ_Δ**	**Φ_d (x10^{-4})**
3a	0.04	0.45
3c	0.03	0.57
ZnPc[a]	0.56	0.23

[a]Data from Ref.[27]

Table 3. Radical-scavenging activity on DPPH radicals (%) of the phthalocyanines.

μM[a]	**3a**	**3b**	**3c**	**Gallic Acid**[c]
25	3.02 ± 0.09 [b]	14.57 ± 0.31 [b]	5.55 ± 0.11 [b]	68.88 ± 0.40 [b]
50	7.79 ± 0.12 [b]	22.58 ± 0.35 [b]	8.46 ± 0.11 [b]	81.53 ± 0.42 [b]
75	9.39 ± 0.15 [b]	30.63 ± 0.32 [b]	15.52 ± 0.19 [b]	87.71 ± 038 [b]
100	14.55 ± 0.19 [b]	32.81 ± 0.40 [b]	22.74 ± 0.15 [b]	90.58 ± 0.50 [b]

[a] Four experiments were performed for all compounds in each experiment in triplicate.

Journal Pre-proofs

[b] Mean values ± SD are shown for triplicate experiments.
[c] Reference compound.

Table 4. Ferrous ions chelating activity (%) of the phthalocyanines.

µM[a]	**3a**	**3b**	**3c**	**EDTA**[c]
25	2.25 ± 0.11 [b]	10.63 ± 0.22 [b]	5.87 ± 0.25 [b]	15.65 ± 0.15 [b]
50	5.41 ± 0.05 [b]	16.52 ± 0.09 [b]	11.52 ± 0.37 [b]	51.42 ± 0.18 [b]
75	8.63 ± 0.07 [b]	21.74 ± 0.76 [b]	17.63 ± 0.24 [b]	82.31 ± 0.08 [b]
100	11.62 ± 0.06 [b]	24.96 ± 0.51 [b]	26.96 ± 0.39 [b]	96.85 ± 0.21 [b]

[a] Four experiments were performed for all compounds in each experiment in triplicate.
[b] Mean values ± SD are shown for triplicate experiments.
[c] Reference compound.

Dear editor,

I have responded to the comments raised by one of the referees and have incorporated suitable revisions. My paper not contains crystal structure determination

Best Wishes

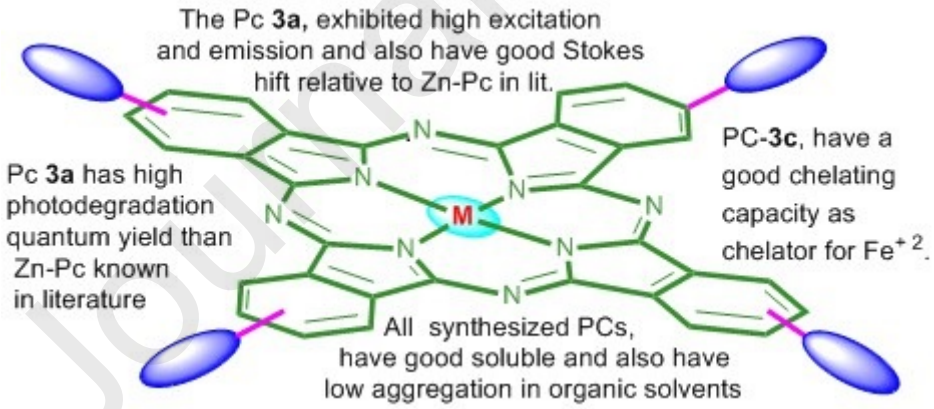

Journal Pre-proofs

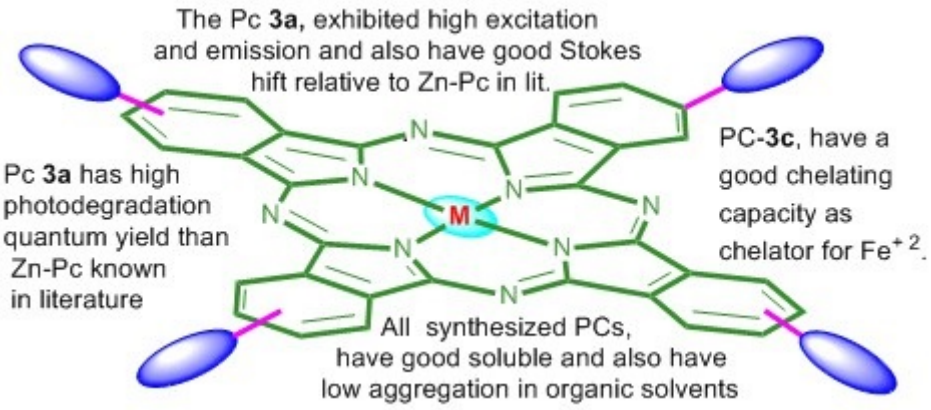

Journal Pre-proofs